

SUPPLEMENTAL FIGURE LEGENDS

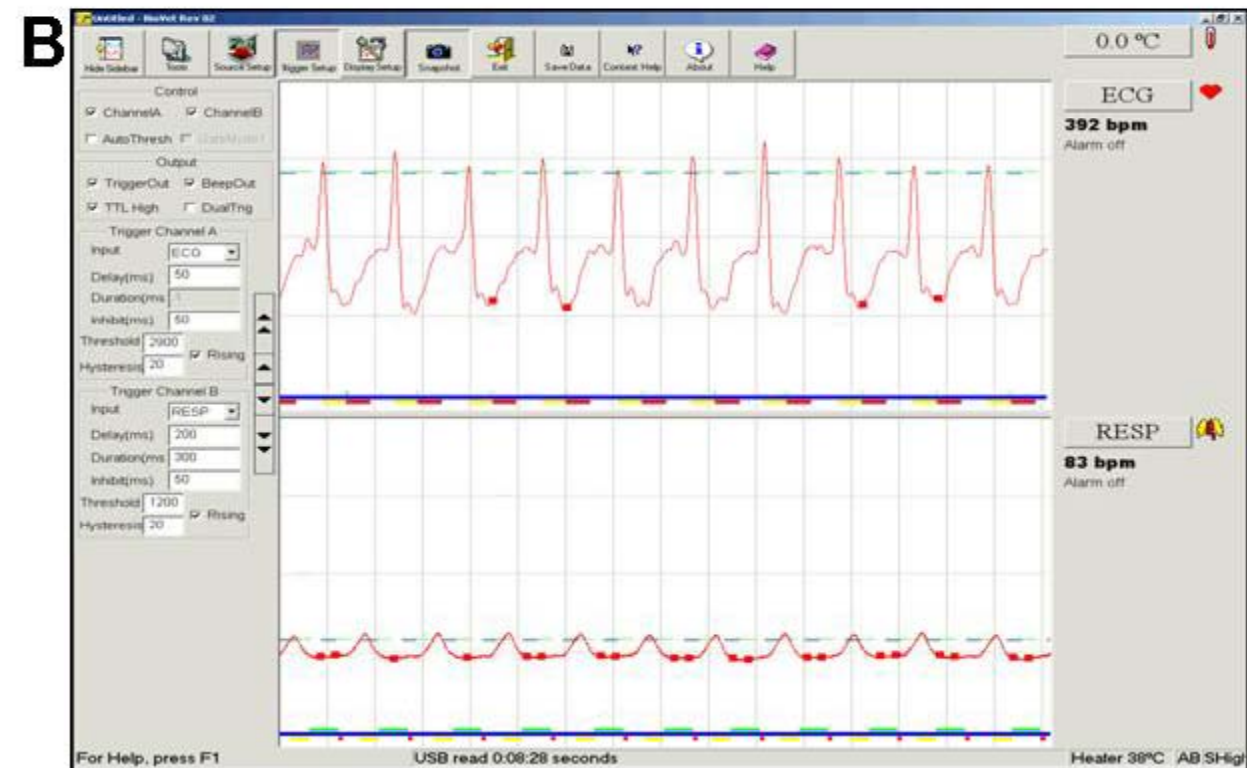
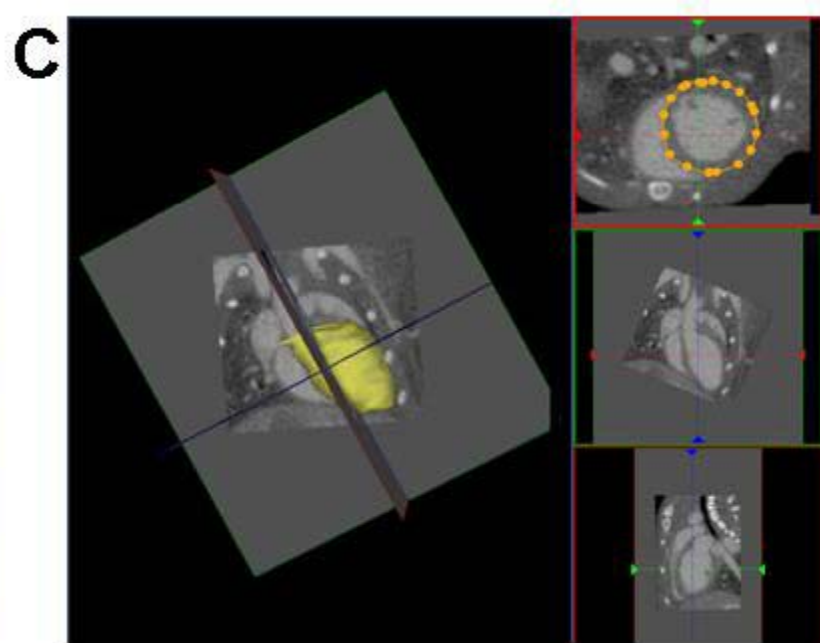
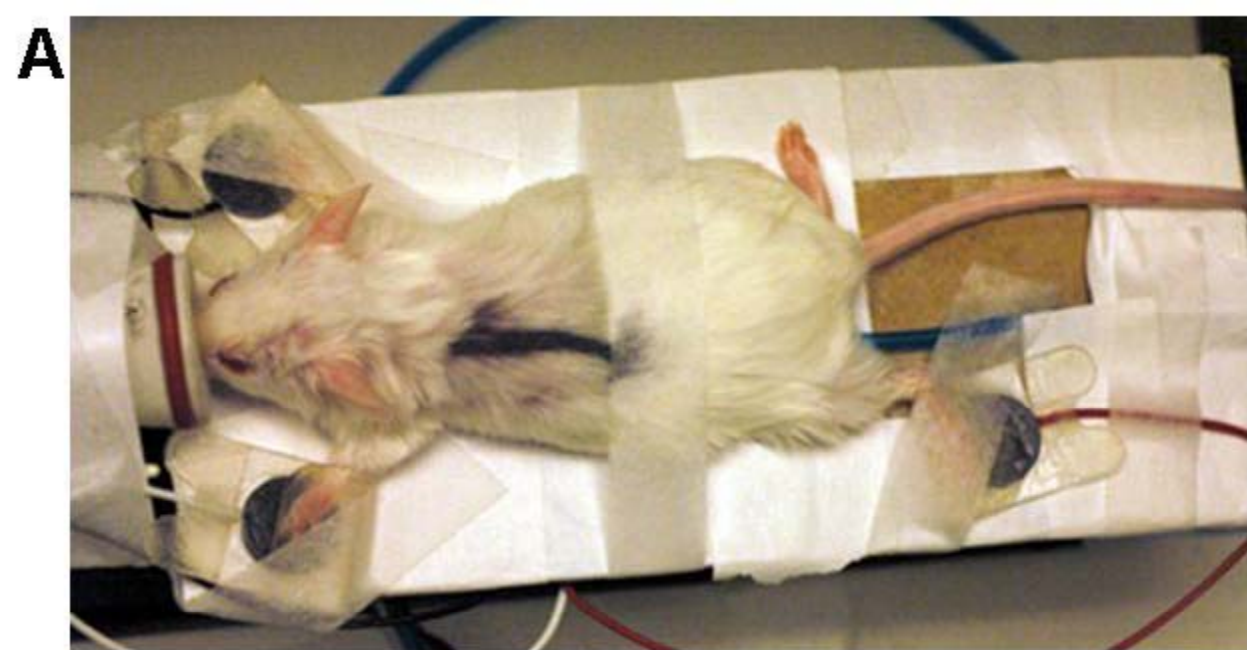
Supplemental Figure 1: *Outline of image acquisition and processing by Micro-CT.* (A) Mouse positioned on CT scanner bed with 3 lead ECG. (B) Screen shot of ECG (top) and respiratory (bottom) tracings. Red squares occurring at the same time in both ECG and respiratory tracings indicate image acquisition points during maximum LV contraction (S') and inspiration. (C) Region of interest (orange dots) created around heart chamber (LV shown). (D) Histogram used to isolate voxels representing chamber volume. (E) Rendered surface of blood within chamber (LV). (F) Representative composite image of cardiac chambers and great vessels.

Supplemental Figure 2: *Quantification of cardiac chamber volumes by Micro-CT.* Representative reconstruction of cardiac chamber volumes in (A) end-systole and (B) end-diastole allowed for extrapolation of chamber volumes and loading conditions during (C) the entire cardiac cycle.

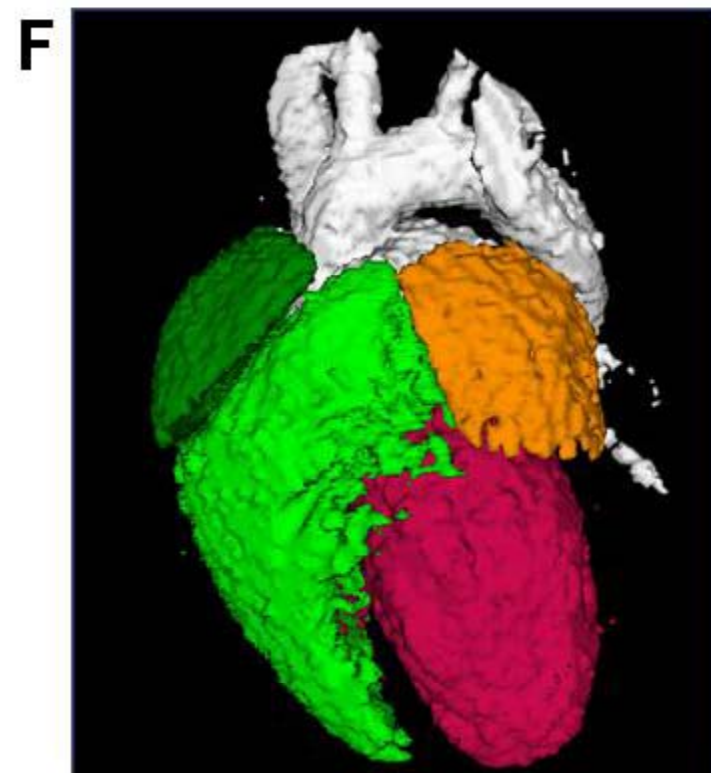
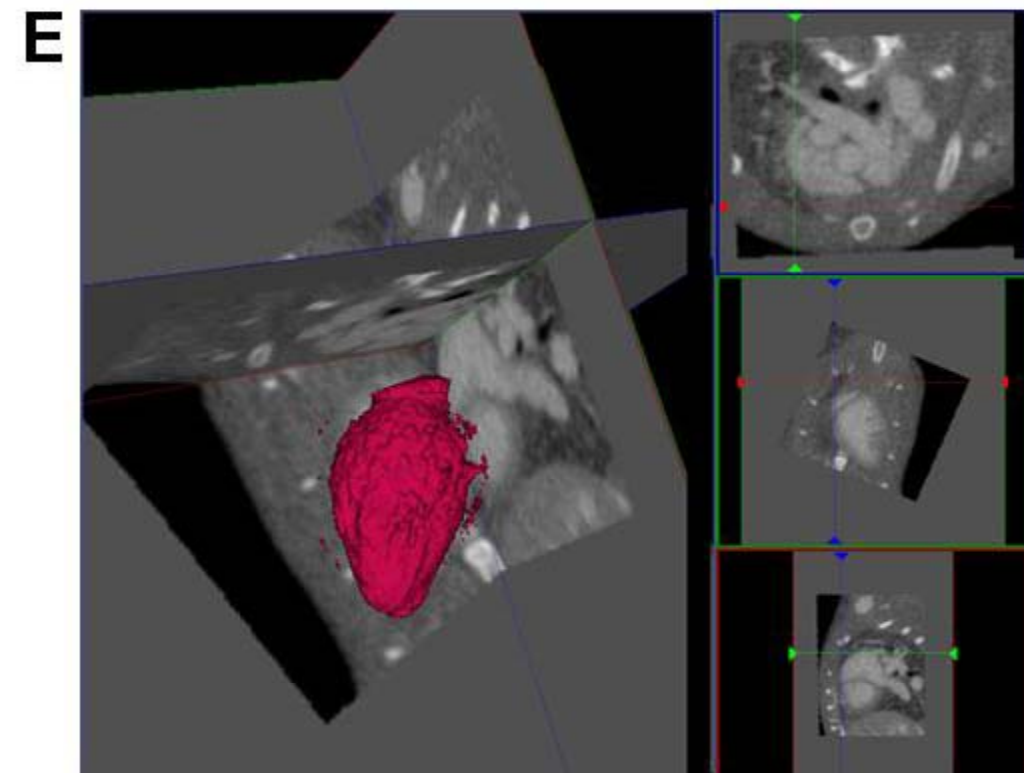
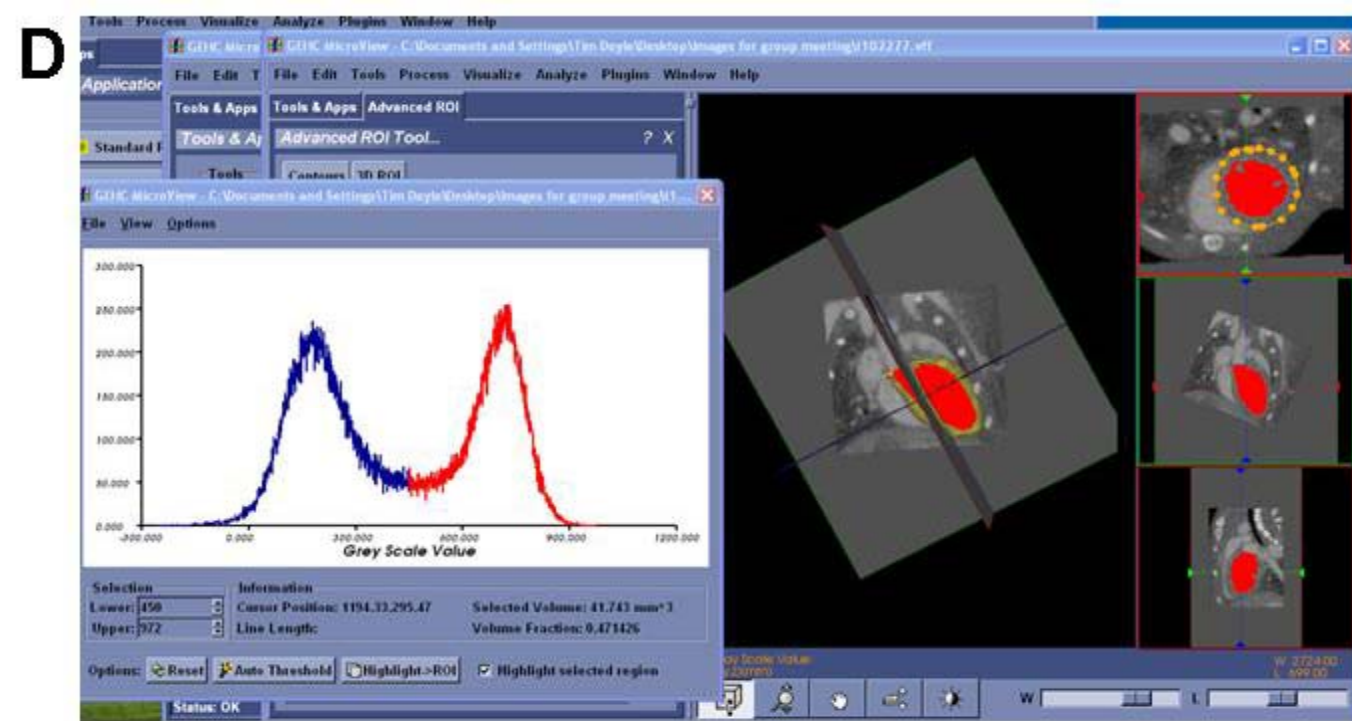
Supplemental Figure 3: *Echocardiographic M-mode traced measurements of ventricular diameters and calculated left ventricular fractional shortening (LVFS).* (A) Representative M-mode traced picture taken at the level of the papillary muscle of a pre-operative heart whereby left ventricular diameters can be measured. Scale bar represents 5 mm. (B) The same heart as in (A) shows extensive dilatation at 12 weeks post-MI. (C-E) A gradual MI-induced increase in ventricular diameters in diastole (LVDD, C), and systole (LVSD, D) translated in a significantly compromised LVFS over a period of 12 weeks as compared to the sham group (Bars represent mean±SE. * represents $P<0.05$ compared to sham group by repeated measurements ANOVA).

Supplemental Figure 4: *Conductance catheter (CC) based assessment of cardiovascular function.* (A) Representative pressure-volume loops of sham (left) and MI (right) animals at 12 weeks post-MI, showing typical right shift indicating increased ventricular dilatation and volumes compared to pre-operative assessment. (B, C) Confirming findings by Micro-CT and echocardiography, extrapolation of pressure-volume loops showed significantly increased ventricular volumes in end-diastole (LVDV, B) and end-systole (LVSV, C) post-MI. (D, E) Cardiac output (CO) as well as stroke work (SW) were both significantly diminished as well. (F) As a confirmatory measure of CHF, the arterial elastance (AE) was also significantly increased at the 12-week post-MI time point. (G) Finally, significantly decompensated MI-induced heart failure was illustrated by a markedly decreased maximum power generated by the left ventricle (Bars represent mean±SE. * represents $P<0.05$ compared to sham group by Student's t-test).

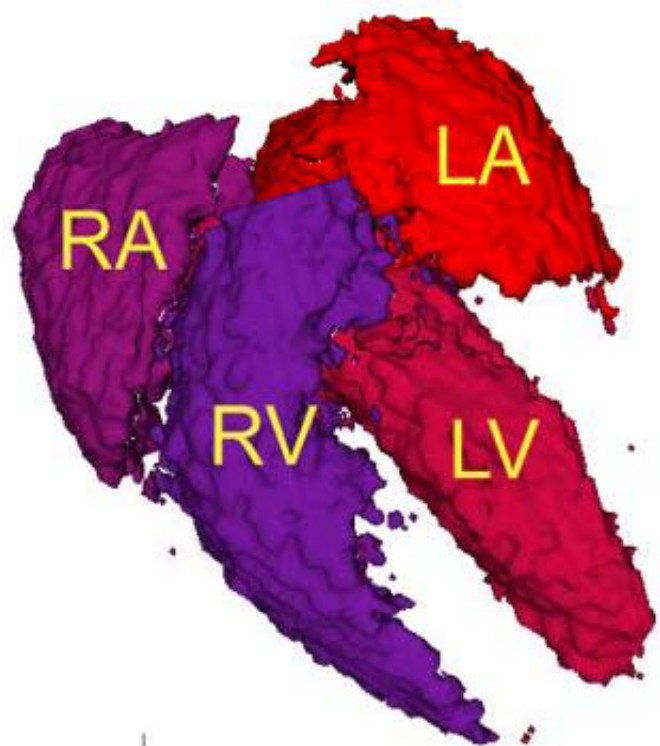
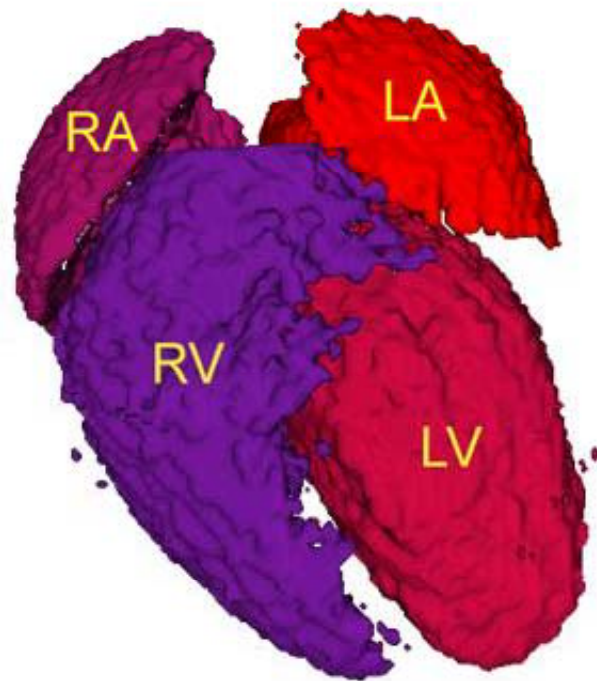
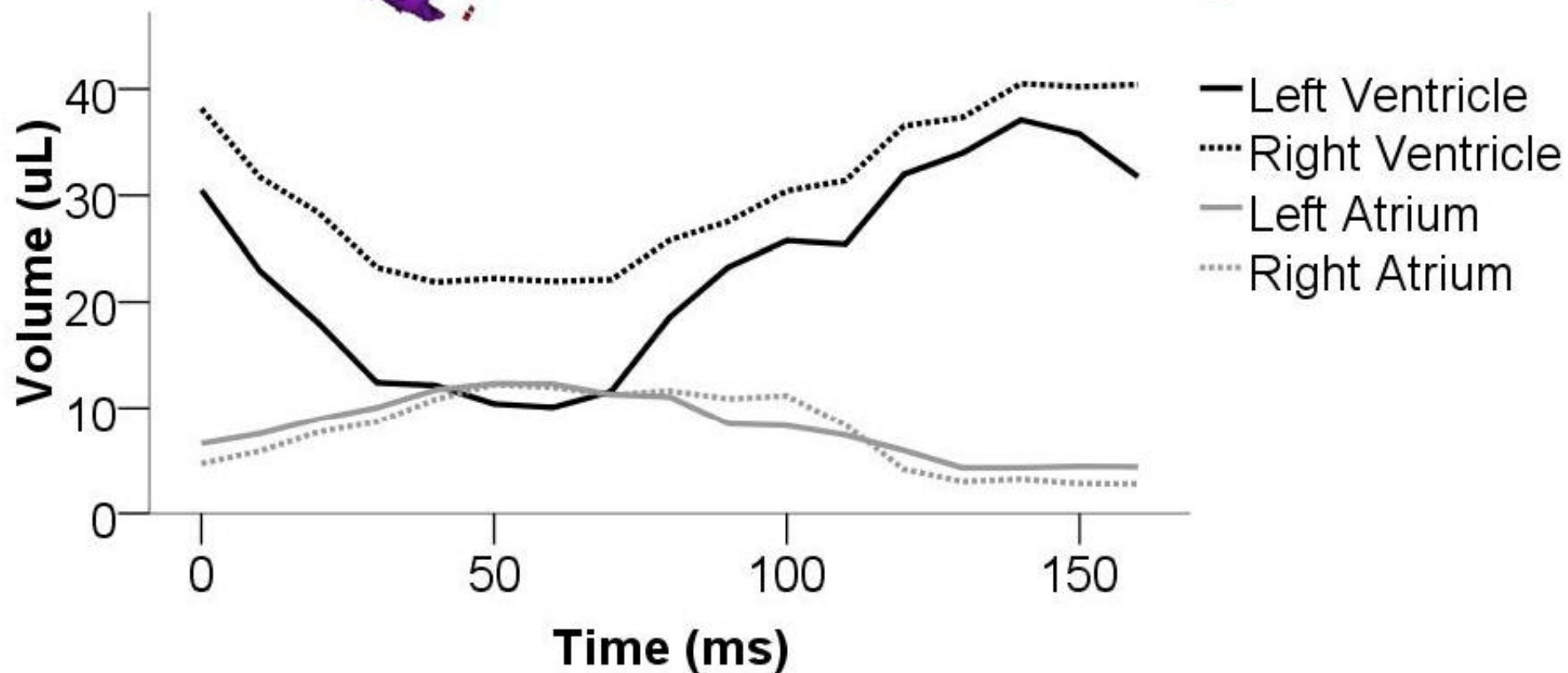
Supplemental Figure 5: *Post-mortem histological analysis confirms in vivo Micro-CT images.* (A, B) Representative heart 12 weeks following sham procedure appears both grossly and histologically normal, corresponding to the *in vivo* images acquired by Micro-CT immediately prior to CC-measurements and sacrifice. (C) By contrast, a representative fixed heart 12 weeks post-infarction shows an aneurysmal, infarcted region and fibrosis on Masson-Trichrome staining (black arrows). (D) Corresponding *in vivo* Micro-CT images from the same heart with the infarcted area marked by yellow arrows clearly resembles the post-mortem images from (C). Scale bars represent 5 mm.



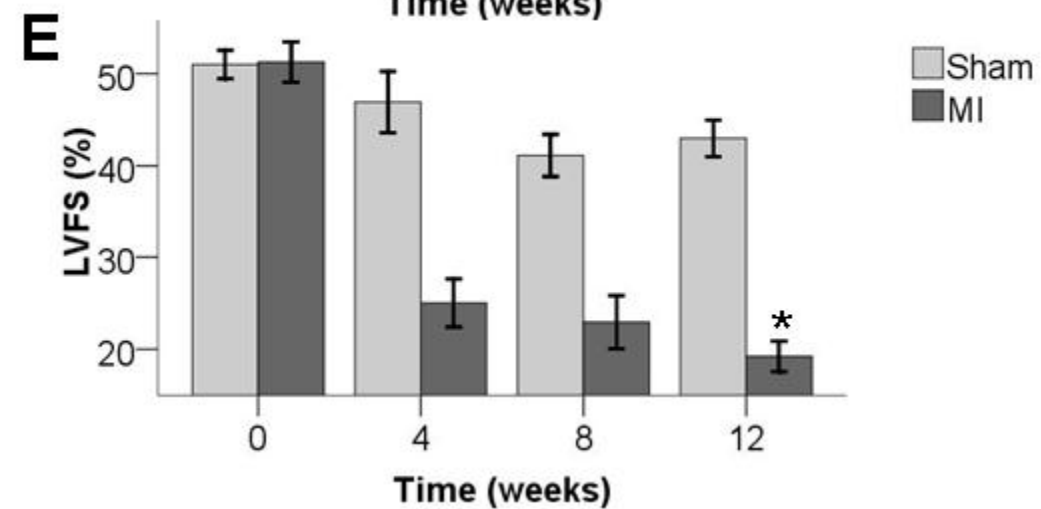
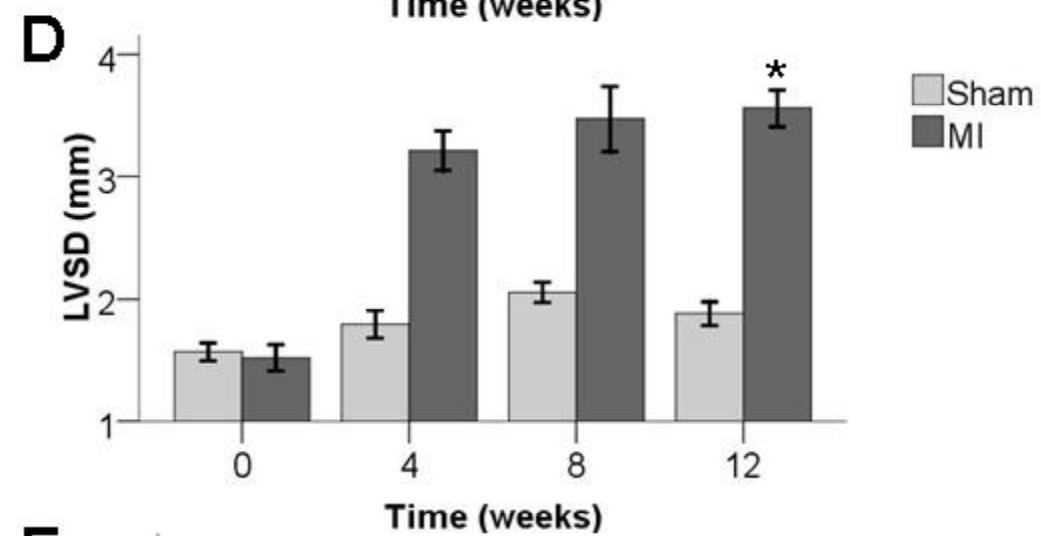
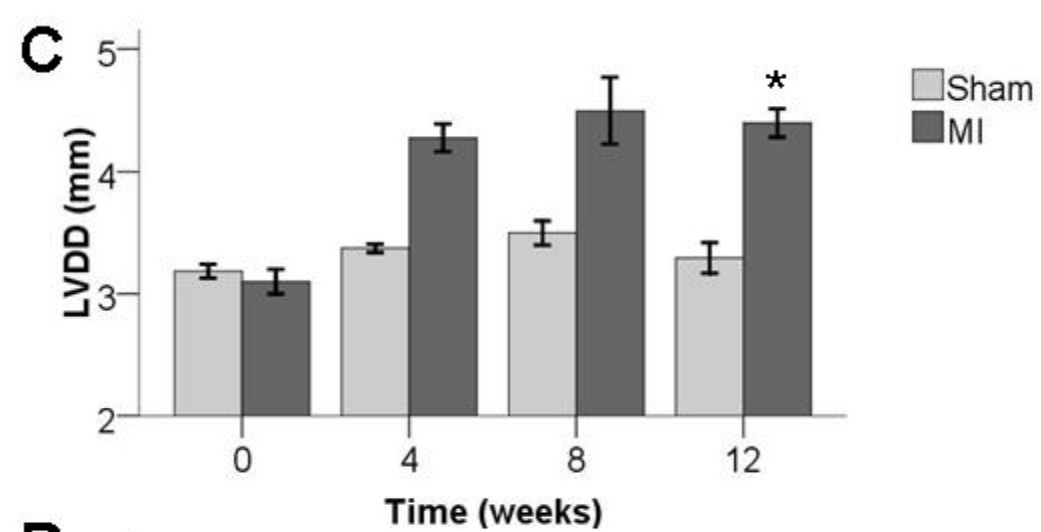
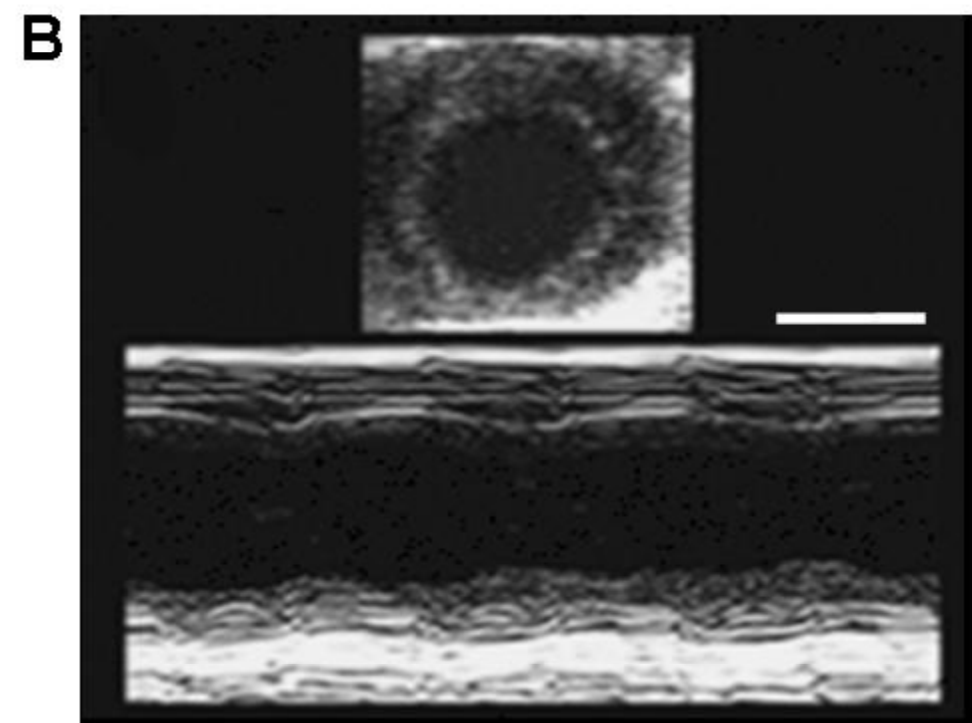
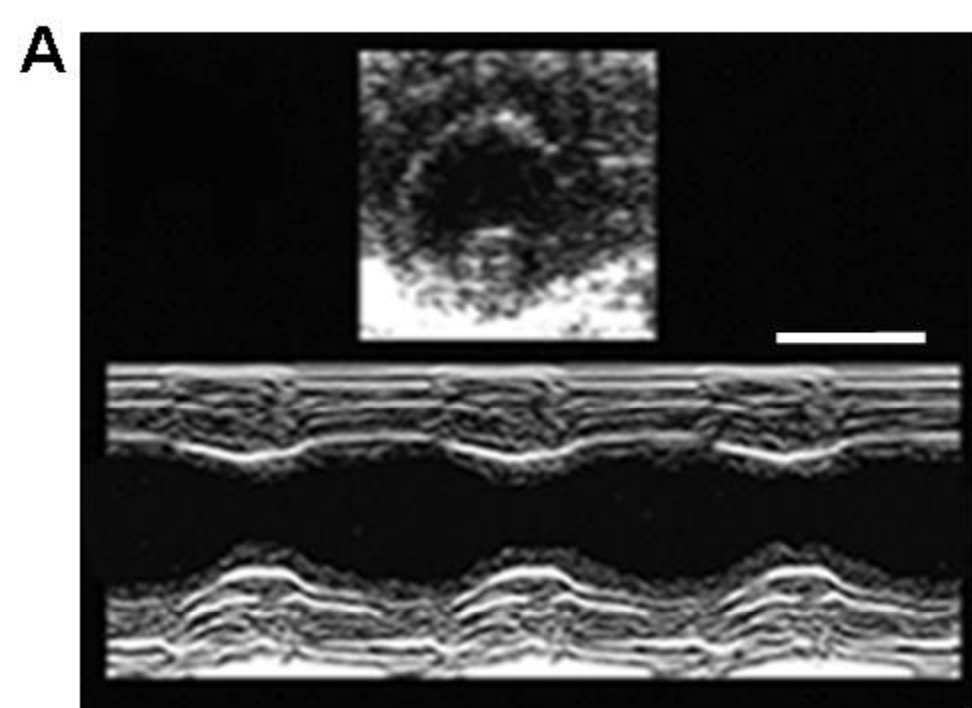
Supplemental Figure 1



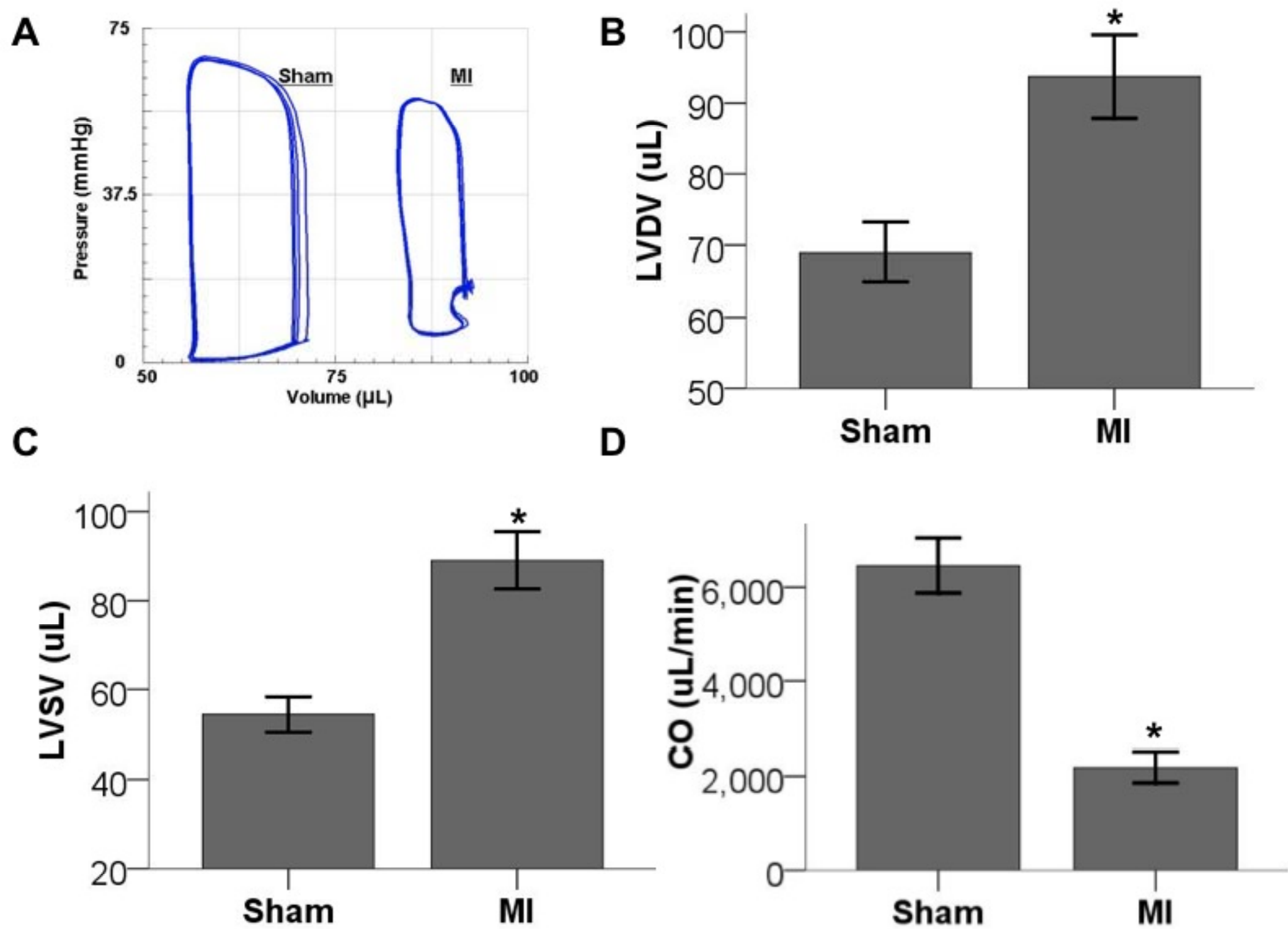
Supplemental Figure 1

A**B****C**

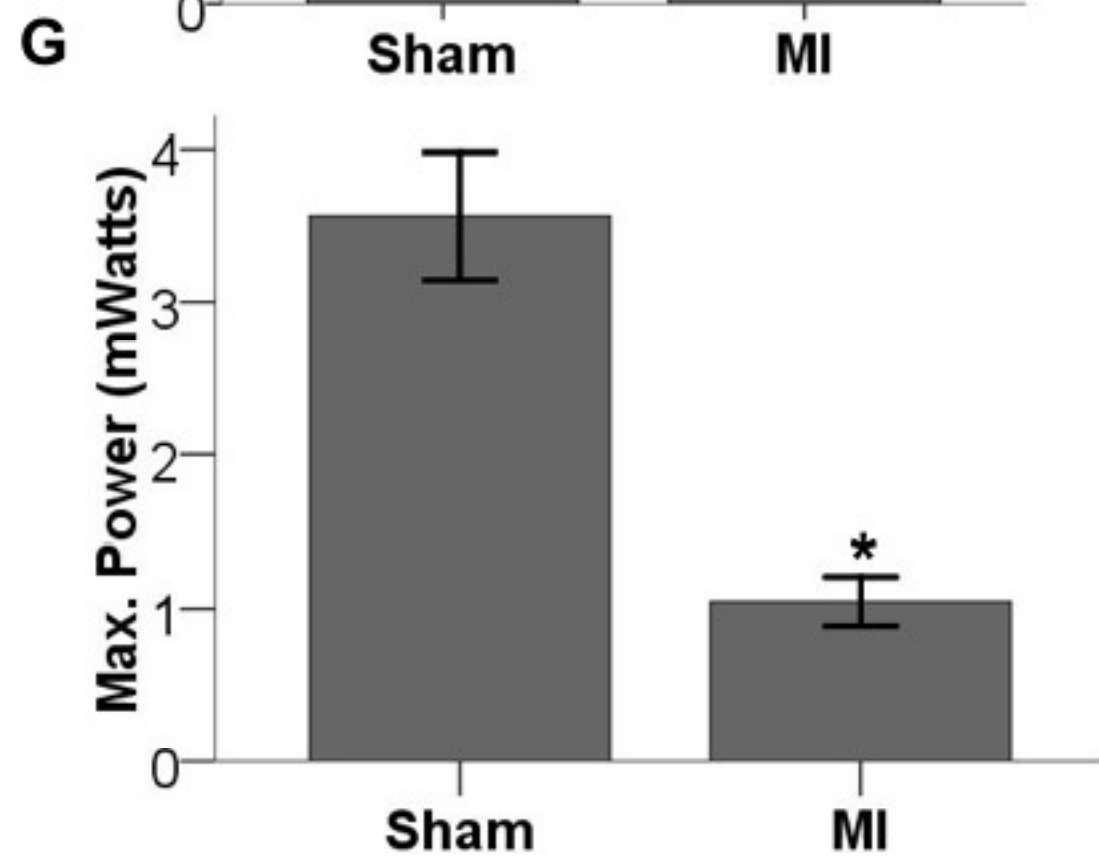
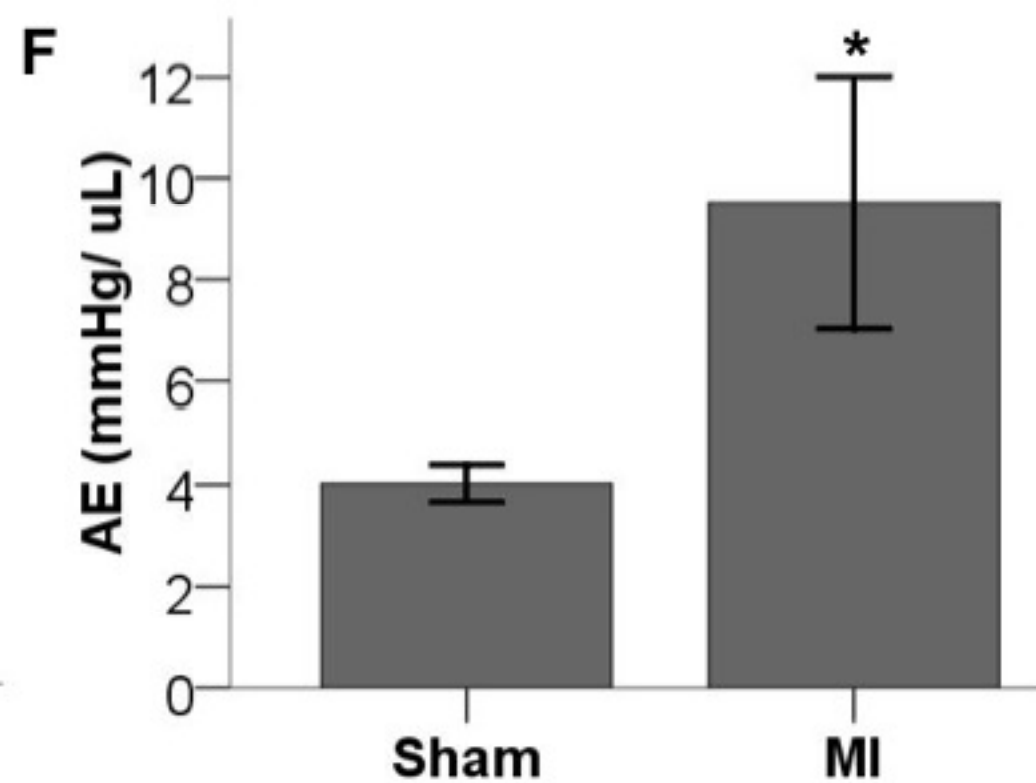
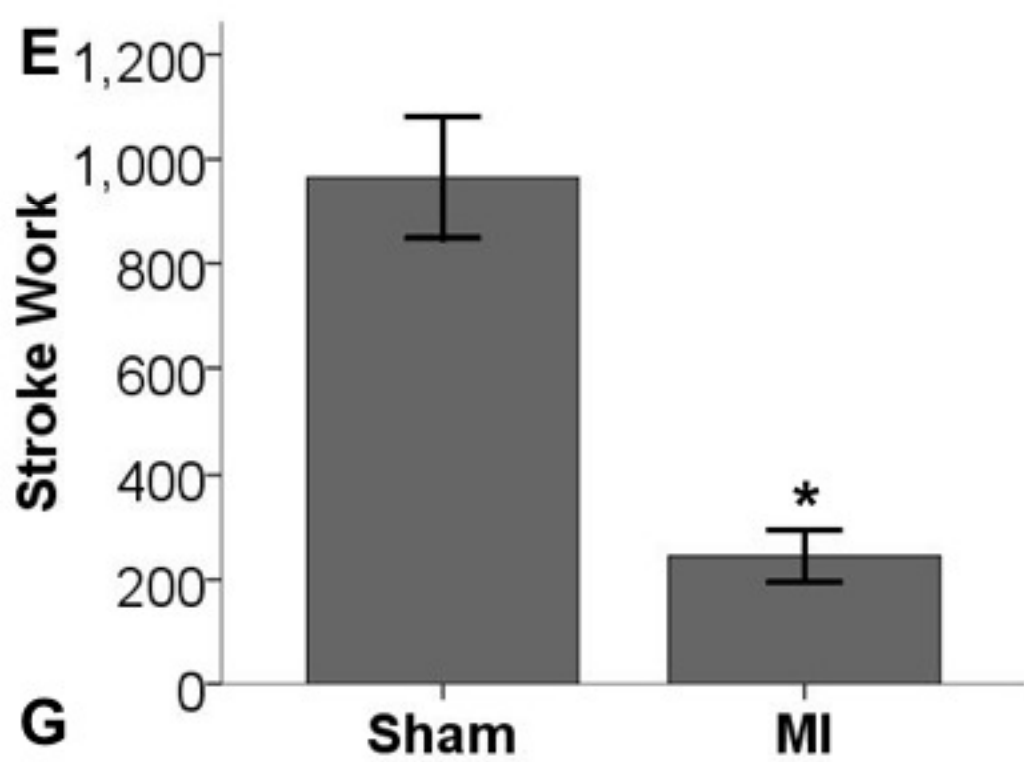
Supplemental Figure 2



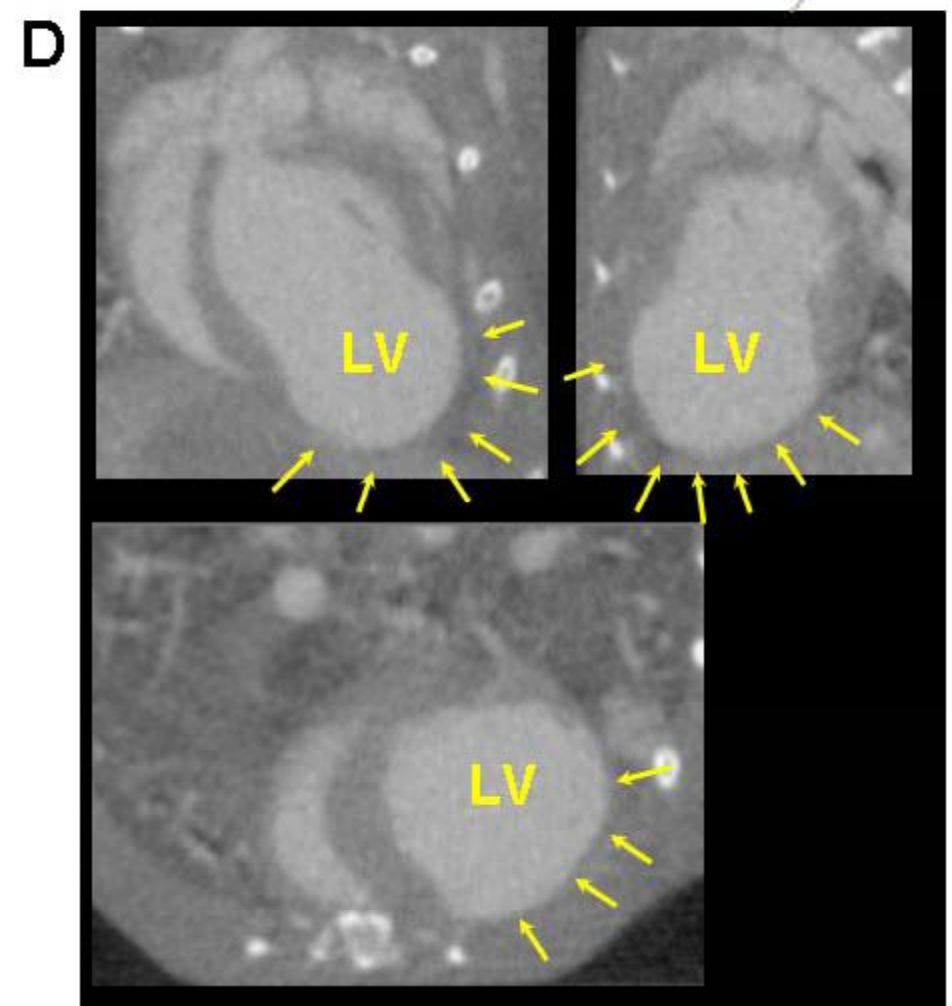
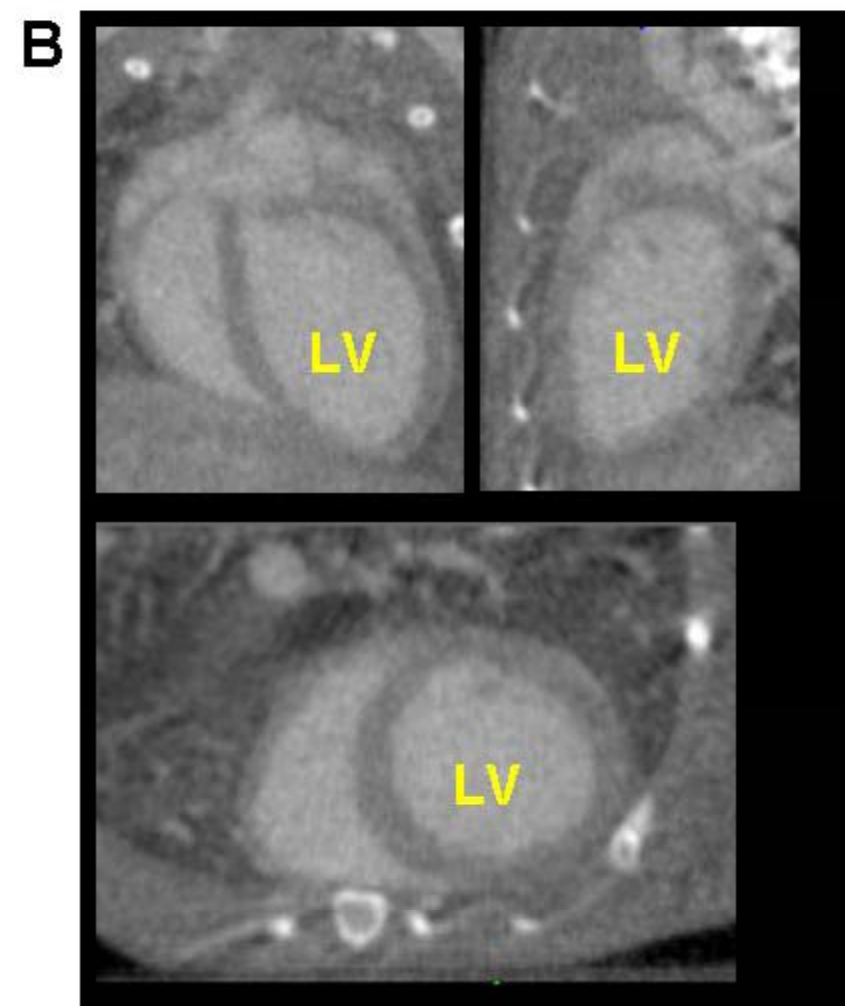
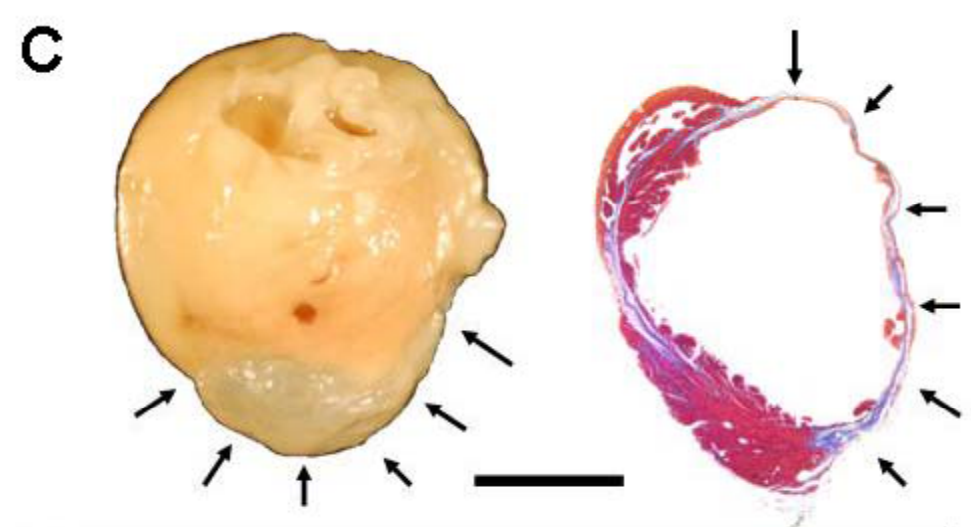
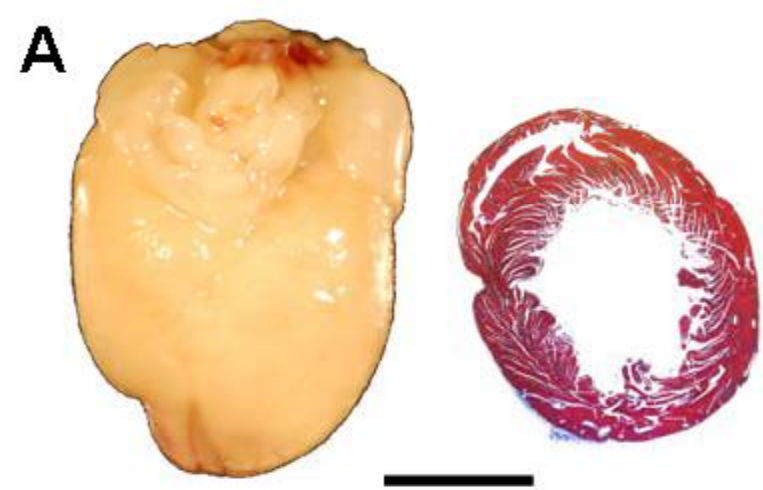
Supplemental Figure 3



Supplemental Figure 4



Supplemental Figure 4



Supplemental Figure 5